Study on the vertical release characteristics of alkali and fluoride in red mud with different compaction degrees

Xiaoduo Ou
Guangxi University
shengjin chen (1810401003@st.gxu.edu.cn)
Guangxi University
Jie Jiang
Guangxi University
Jinxi Qin
guangxi xinfazhan communication group co., ltd.
Zhijie Tan
guangxi hualan geotechnical engineering co.,ltd.
Wei Su
Tongji University

Research Article

Keywords: Bayer red mud, Alkali pollution, Fluoride pollution, Vertical leaching, Release characteristics

Posted Date: February 23rd, 2022

DOI: https://doi.org/10.21203/rs.3.rs-1326798/v1

Abstract

In this study, the vertical migration and release characteristics of alkali and fluoride in Bayer red mud with different compaction degrees were investigated by conducting constant head vertical leaching tests. The experimental results showed that the breakthrough time of leaching liquid across the red mud column increased with the increase of compaction degree, the alkali and fluoride concentrations of the leaching outflow decreased fast as the compaction degree of red mud column increased, as well as the time required to reach the leaching equilibrium. Moreover, for all the leaching red mud columns, the cumulative release of alkali and fluorine from the increased with the increase of leaching durations. However, the total release of major pollutants decreased with the increase of red mud compactness. After leaching, the soluble alkali and water-soluble fluorine (Ws-F) residual in the red mud gradually increased from top to bottom along the leaching column, and at the identical depth, the higher the compactness of the leaching column, the greater the soluble alkali and water-soluble fluorine (Ws-F) remaining in the column after leaching. These phenomena indicated that improving the compactness can effectively slow down the release of main pollutants in the red mud. The results were expected to provide a scientific basis for the prevention and control of alkali and fluoride pollutants in red mud yard.

1 Introduction

Red mud is a kind of solid wastes produced in the process of alumina industrial production (Kong et al., 2017). About 1–2 tons of red mud will be produced for one ton of alumina. By 2018, the global red mud stockpile was reported to reach 4.6 billion tons and the annual output about 200 million tons (Xue et al., 2019). According to the production process, red mud can be classified as Bayer process red mud, sintering process red mud and combined process red mud. Bayer process red mud accounts for 95% of the total amount in the world (Power et al., 2011). A large amount of piled red mud poses a serious threat to the environment, especially the harm caused by the leakage of pollutants into water（Jha et al., 2008; Ding et al., 2018; Bombik et al., 2020）.

During the alumina production process, a large number of NaOH and certain kinds of fluorine-rich raw materials are needed, resulting in the red mud containing alkali, fluoride and other pollutants. Therefore, the red mud yard becomes the source of alkali pollution and fluorine pollution to the surrounding environment. Researches revealed that there are two kinds of alkali in red mud, namely soluble alkali and non-soluble alkali (Zhu et al. 2015; Xue et al. 2016a), also known as free alkali and bound alkali. Soluble alkali mainly includes sodium hydroxide, sodium carbonate, sodium bicarbonate, sodium aluminate dihydrate, sodium silicate, potassium hydroxide and potassium carbonate, etc. (Xue et al. 2017); Non-soluble alkali mainly includes sodalite, nepheline, hydrated garnet, tricalcium aluminate, and calcite, etc. The soluble alkali is soluble in water and thus has significantly negative impact on the environment. Fluorine can be divided into water-soluble fluorine (Ws-F), exchangeable fluorine (Es-F), iron manganese bound fluorine (Fe/Mn-F), organic bound fluorine (Or-F) and residual fluorine (Res-F) (Muravyeva et al., 2014; Yuan et al., 2008). Tessier five-step extraction method was usually used for fluoride extraction (Tessier a et al. 1979; Xie et al., 1999; Wu et al. 2002). Water soluble fluorine (Zhang et al. 2020; Gao,

2013) and Es-F can be dissolved in water and thus have a great impact on the water environment. The influence of fluorine pollution depends not only on the total content of fluoride, but also on the form of fluorine. The greater the content of Ws-F and Es-F, the greater the negative influence on the environment.

When experiencing rainfall, pollutants will be released from the newly stacked red mud by the surface runoff in a short time. The Chinese standard GB/T 51238 – 2018 has regulated the requirements for compaction degree of stacked red mud. However, the actual compactness of the red mud is commonly found to fail to meet the specification due to mechanical compaction operation and other uncertain factors. For this reason, during the rainy seasons in the south area of the nation, rainwater will have different effects on pollutants released from red mud in the vertical runoff direction under different compaction conditions of stacked red mud. Therefore, in this work, constant head dynamic leaching test was employed to study the release and migration characteristics and the change of occurrence content of pollutants in the process of vertical seepage in red mud with different compaction degrees, so as to clarify the influence of different compactness on the release and migration of red mud pollutants. Through the above research, the environmental effects of water infiltration on red mud under different compaction conditions are clarified. Based on which, the scientific basis and technical guidance are provided for the prevention and control of main pollutants in red mud storage yard.

2 Materials And Methodology

2.1 Raw Materials

2.1.1 Red mud

The red mud used was obtained from the red mud yard of Xinfa Aluminum Co., Ltd. The main chemical components of red mud are Fe_2O_3, Al_2O_3, SiO_2, CaO, etc, note that the red mud contains 9.21% Na_2O, which can provide hydroxyl during its hydration process. The main mineral facies of red mud are Hematite, Andradite, Cancrinite, etc.

According to the field investigation, filter cake method is adopted to the stockpile the red mud in the storage yard (Chinese standard GB/T 51238 – 2018). The piling height of the red mud ranges from 50 to 100 cm (Cao, 2017). The maximum dry density of the tested red mud is 1.49 g/cm^3. Based on this density, four compactness, namely compaction coefficient λ_c = 0.8, 0.85, 0.88 and 0.9 were selected in this study, to clarify the influence of the compactness on the vertical migration of main pollutants, the release characteristics of alkali and fluoride in red mud.

2.2 Test methods

2.2.1 Apparatus

Referring to Guo (2019), a series of constant head leaching devices were designed. The structural diagram of the leaching device is shown in Fig. 1, PVC pipe with an outer diameter of 110 mm (the actual

inner diameter is 106 mm) was used as the cell to accommodate the red mud column. The top of the soil column was connected to the liquid supply bottle and the bottom to the collecting bottle. After filling the PVC pipe with red mud, a peristaltic pump was used to continuously add deionized water from the supply bottle to the leaching column. A hole 10 cm away from the soil bottom was kept open as an overflow hole to ensure that the overlying water head in each leaching column is the same and maintained at 10 cm. At the same time, a hole was set at the bottom outlet to collect the leachate into the liquid collection bottle for daily sampling.

2.2.2 Sampling design

(1) Leachate sampling

The daily leachate for each leachate column was collected in the liquid collection bottle. After shaking up, 50 mL of the collected leachate samples were taken using a 50 mL centrifugal tube for water sample analysis. Each time, two tubes of leachate sample were taken as a parallel group and the average value was taken.

(2) Red mud sampling after leaching

At the end of the leaching test, the leachate in the column was drained and the upper quartz sand and absorbent cotton were removed. The PVC column was cut with a cutting machine. The red mud column was sampled at 0, 5, 10, 15, 20, 25, 30 and 35 cm along the height from the top surface.

2.2.4 Method of measurement

(1) Leaching rate measurement

During the leaching test, a 100 ml measuring cylinder was used to collect the filtered solution for half an hour after the leachate outflow velocity became uniform. The collected volume was measured and the filtered velocity was calculated. This measurement was carried out for three times and the average value was taken.

(2) Total effluent from the leaching column

A measuring cylinder was used to measure the total volume of filtrated liquid in the collecting bottle.

(3) Soluble alkali and fluoride content in red mud after leaching

According to Chinese standard GB/T 51238 – 2018, the alkali content in red mud was calculated by Na_2O. therefore, the alkali concentration in the leaching liquid was characterized by Na^+ concentration, and the Na^+ concentration was measured by Flame Photometer (Li, 2012; Yang, 2015).

The determination of the total content of fluorine was conducted according to Chinese standard GB/T22104-2008. The occurrence forms of fluorine were extracted by Tessier five-step extraction method (Tessier A et al., 1979; Yuan et al., 2008; Zhang et al., 2020).

3 Results And Discussions

3.1 Leaching time and rate

Figure 2 shows the process of the leaching time and rate of leaching columns with different the compactness. It can be observed that the leaching time increased with the increase of the compaction degree of the red mud column. In the leachate column $\lambda_c = 0.80$, the leachate flowed out of the sample at the 6.45th hour after the beginning of leaching, while in the leachate column $\lambda_c = 0.90$, it took 24.13 hours for the leachate to flow out after the beginning of leaching. The increase of the compactness of the red mud increased the leaching time mainly due to the decrease of the soil permeability. Meanwhile, the results also showed that under the condition of $\lambda_c = 0.90$, it took 24.13 hours of continuous leaching for alkali, fluoride and other pollutants in red mud to infiltrate with the seepage fluid and migrate to deeper soil. For the case of $\lambda_c = 0.80$, the steady outflow rate of leachate was 63.6 mL/h, while for $\lambda_c = 0.90$, the steady outflow rate of leachate was only 15.2 mL/h. The reason could be that the number of pores in red mud with high compactness leachate column are smaller, and so was the permeability coefficient. Thus, the seepage flow was smaller.

According to the test, the height of the leaching column with 80% compactness before leaching was 40.6 cm, and the height after leaching was 38.5 cm, with the maximum settlement of 2.1 cm. The height of the leaching column with 90% compactness before leaching was 36.3 cm, and the height after leaching was 36.1 cm, with the minimum settlement of 0.2 cm. The reasons for this phenomenon could be as follows: on the one hand, the consolidation settlement of red mud was induced by the increase in the self-weight due to saturation during the leaching process; On the other hand, after leaching, the pore water pressure of red clay decreased and the effective stress increased, leading to the settlement. Therefore, it can be inferred that the red clay with small compactness is prone to settlement after rainfall, which would have negative impact on the surface transportation operation of the yard and the stability of the slope at the edge of the yard.

3.2 pH variation of the leachate

The variation of the pH of the leachate from red mud columns with different compactness with the leaching time is shown in Fig. 3. According to the curves, except for the leachate column with compactness of 90%, the pH value increased slowly with the increase of the leaching time, and then gradually reached the peak value after the leaching for 7d, and then enters a declining stage, and becomes stable after the leaching for 15d. However, the pH value of the leachate of the leaching column with 90% compactness decreased slowly with the increase of the leaching days, and finally stabilized after 15 d. With the increase of compactness, the pH value of filtrate decreased. The pH value of leaching solution with compactness of 80% was up to 11.04, while that of leaching column with compactness of 90% was only 10.61 at the beginning, and then decreased until reaching stable at around 10.0. The reason for this phenomenon could be that, the lower the compactness, the larger the pore size in the soil,

the larger the contact area between water and particles, the more OH^-, HCO_3^-, CO_3^{2-} plasma released into the soil, and the higher the pH value.

3.3 Release characteristics of main pollutants in leachate

3.3.1 Alkali release characteristic

Figure 4 (a) shows the evolution of alkali concentration of the leachate with the increase of leaching time. It can be seen from the figure that the evolution of alkali concentration with time for all the leaching columns was consistent. With the increase of leachate time, there was constant contact between leachate water and the red mud between along the leachate channels in each soil column, soluble alkali was thus constantly released, and the concentration gradually decreased with time. By comparing, the concentration of alkali in the column with low compactness was found to decrease faster and the time to reach stable was faster. Since the lower the compactness was, the more leaching amount was obtained, the soluble alkali could be taken away quickly in a short time. For the column with high compactness, the contact between the red mud and the leachate was not sufficient due to the small pore space, which affected the release rate of the leachate. However, as the leachate volume was small, the alkali concentration of the leachate became large. After 21 days of leaching, the final alkali concentration of leachate in cases of λ_c = 0.8, 0.85, 0.88 and 0.9 were 32, 457, 691 and 832 mg/L, respectively, and the alkali concentration of in each case exceeded the upper limit of primary and secondary groundwater water (i.e. 200 mg/L).

Figure 4 (b) shows the cumulative release amount of alkali. It can be seen from the curves that the cumulative release amount of alkali in each leaching column increased gradually with the leaching time. After fitting the test data, the exponential growth trend was observed with correlation coefficients over 0.97. It can be further seen from Fig. 4 (b) that the cumulative release curve of alkali of each red mud column was basically consistent. With the increase of the initial compactness, the cumulative release increased. In addition, the cumulative release of alkali in cases of λ_c = 0.8, 0.85, 0.88 and 0.9 at 21th day were 23909.62, 20805.62, 16183.78 and 14061.66 mg, respectively, indicating that the improvement of the compactness can significantly delay the release of alkali from red mud.

3.3.2 Fluorine release characteristics

Figure 5 (a) shows the change of fluoride concentration in the leachate of each leaching column with time. In the cases of λ_c = 0.80 and 0.85, the development of leachate concentration were basically consistent, while the fluoride concentration of the leachate for λ_c = 0.88 and 0.90 fluctuated. The relationship between the fluoride concentration in the exudate and the compaction coefficient is consistent with that with respect to alkali. The initial concentration of leachate in each group was more than 50 mg/L, which was far higher than the upper limit of fluoride concentration in surface water of 1.5 mg/L stipulated by Chinese Standard GB/T14848-2017, At the end of 21-day leaching test, the final fluoride concentration values for λ_c = 0.8, 0.85, 0.88 and 0.9 were 3.46, 7.23, 20.66 and 27.45 mg/L, respectively, which were all higher than the limits of fluoride in various groundwater water.

Figure 5 (b) shows the cumulative release amount of fluoride from the red mud columns. It can be seen from the figure that the cumulative release amount of fluoride from each leaching column increased gradually with the leaching time. After fitting the test data, exponential growth trends were obtained with correlation coefficients all over 0.93. It can be seen from Fig. 5 (b) that the cumulative release of fluoride decreased with the increase of compactness. The cumulative release of fluoride at the 21th leaching under the compactness of λ_c = 0.8, 0.85, 0.88 and 0.9 were 463.57, 440.90, 406.48 and 388.60 mg, respectively. Under the same conditions, increasing of compactness can significantly reduce the fluoride release from red mud.

3.4 Occurrence and vertical distribution characteristics of pollutants along the red mud column after leaching

3.4.1 Alkali distribution characteristics

Figure 6 shows the change of soluble alkali content in red mud along the height after leaching. It is shown that after 21 days of leaching, the content of soluble alkali in the red mud increased gradually from the top surface to the bottom in the leached columns with different compactness. These phenomena could be attributed to that: since the red mud columns were leached from top to bottom, the adhesive soluble alkali in the upper part of red mud is released to the water and transported downwards with the filtrate. While during the infiltrate, since the red mud particle has a large specific surface area, part of the soluble alkali could be adsorbed by the lower part of red mud, lead to the concentrating of soluble alkali in the lower part of soil column. As can be seen from Fig. 6, the higher the compactness of red mud column, the higher the soluble alkali content at the same depth of the column after leaching, indicating that the increasing compactness of red mud can significantly hinder the release of soluble alkali.

3.4.2 Fluorine occurrence and distribution characteristics

The Tessier five-step extraction method was used to extract fluoride from the red mud at different depths after leaching. Figure 7 shows the content distribution of Ws-F and Es-F along the column height.

It can be seen from Fig. 7 (a) that, the Ws-F content in the red mud after leaching was significantly reduced under the condition of the low compactness, and there was no significant difference in the distribution along the leached column, with the content of 12 mg/kg. In the case of low compactness, the infiltrating water was expected to be in complete contact with the red mud and all soluble fluorine was thus released. This is also the main reason for the lowest concentration of fluoride observed for the column with 80% compactness in Section 3.4.2. The red mud column with relatively high compactness can effectively prevent the rapid release of Ws-F, so the Ws-F increased along the height from top to bottom, and the greater the compactness, the more significance the increasing trend. It can be observed from Fig. 7 (b) that the Es-F under different compactness conditions did not show relevant laws. The Es-F concent of each column was in the range of 5.0 ~ 8.0 mg/kg. The reason for this phenomenon could be that Es-F was a fluorine anion adsorbed on the exchangeable positive charge of clay particles, organic

matter particles and hydrate oxides through electrostatic attraction. Since the leachate contained a large number of ions, during the leaching process, Es-F can be exchanged from red mud by ion exchange (Gomez et al., 2000; Yuan et al., 2008).

4 Conclusions

The vertical migration and release characteristics of main pollutants in red mud columns with different initial compaction degrees were investigated by dynamic leaching test. Through the research, the following conclusions are drawn:

(1) The dynamic leaching test shows that the leaching time increased with the increase of the compaction degree of the red mud column, but the leaching rate decreased with the increase of the compaction degree. The increase of compaction degree can help reducing the sedimentation of the leached column.

(2) The leaching concentration of alkali and fluoride for red mud column with low compaction degree decreased faster and reached stable faster. This is because the lower the compactness is, the more leaching amount is, and soluble alkali and fluoride can be taken away faster in a short time. For the column with high compaction degree, the contact between the red mud and the leachate was not sufficient due to the small pore space in soil, which affected the release rate.

(3) The cumulative release amounts of alkali and fluorine in each leaching test increased with the increase of leaching time. At the end of 21-day leaching, the total release amounts of alkali from the red mud columns with compactness of λ_c = 0.8, 0.85, 0.88 and 0.9 were 23909.62, 20805.62, 16183.78 and 14061.66 mg, respectively; those of the release amounts of fluoride were 463.57, 449.90, 406.48 and 388.60 mg, respectively. These indicated that under the same conditions, the increase of the compactness can significantly reduce the release of soluble alkali and fluoride.

(4) After leaching, soluble alkali and Ws-F in the red mud gradually increased from top to bottom along the leaching column. At the same depth, the higher the compaction degree, the greater the soluble alkali and Ws-F content after leaching, indicating that improving the compaction degree can effectively slow down the release of main pollutants in the red mud. Under the same leaching time and conditions, the release of alkali and fluoride can be reduced when the compactness is 90%, When the compactness decreases, the release and migration of alkali and fluoride in red mud in vertical runoff will be aggravated.

Declarations

Author contribution Xiaoduo Ou: Conceptualization, Funding acquisition. Shengjin Chen: Investigation, Writing – original & editing. Jie Jiang: Methodology, Supervision. Jinxi Qin: Data curation, Writing – review. Zhijie Tan: Formal analysis. Wei Su: Software.

Funding This research is financially supported by the National Natural Science Foundation of China (Grant No. 51768006 and Grant No. 51978179), the Key R&D Program of Guangxi Province (Grant No. AB19245018), and the Technical Innovation Guidance Program of Guangxi Province (Grant No. AC20238002).

Availability of data and materials All data generated or analysed during this study are included in this published article.

Ethics approval and consent to participate Not applicable.

Consent for publication Not applicable.

Competing interests The authors declare no competing interests

References

1. Bryan R, Simms P, Verburg R (2010) Coupling oxidation to transient drying during multilayer deposition of thickened gold tailings[J]. Miner Eng 23(14):1101–1112
2. Tsamo C, Djomou Djonga PN, Dangwang Dikdim JM, Kamga R (2018) Kinetic and Equilibrium Studies of Cr(VI), Cu(II) and Pb(II) Removal from Aqueous Solution Using Red Mud, a Low-Cost Adsorbent [J]. Arab J Sci Eng 43(5):2353–2368
3. Chen Y (2018) Application of Red Mud Resources in Highway Engineering. Shan dong. Shandong University Press, China
4. Chinese Standard (2008) Code for construction and quality acceptance of road works in city and town. CJJ 1-2008. Chinese Standard, Beijing
5. Chinese Standard (2015) Specifications for design of highway subgrades. JTG D30-2015. Chinese Standard, Beijing
6. Chinese Standard (2020) Specification for highway geotechnical test. JTG 3430 – 2020. Chinese Standard, Beijing
7. Delhimi N, Rezai B (2018) Characterization studies of red mud modification processes as adsorbent for enhancing ferricyanide removal. J Environ Manage 206 JAN 15:266–275
8. Gomez AJL, Giraldez I, Sanchez-Rodas D, Morales E (2000) Comparison of the feasibility of three extraction procedures for trace metal partitioning in sediments from south-west spain. Sci Total Environ 246(2–3):271–283
9. Hedlund HGL, Gustavsson, Soderman A (2012) Tailings dewatering and filtering using the metso vpa filter[C]. 26th International Mineral Processing Congress, pp 1986–1991
10. Hua Y, Heal KV, Friesl-Hanl W (2017) The use of red mud as an immobiliser for metal/metalloid-contaminated soil: A review[J].Journal of Hazardous Materials,325
11. Li G, Ye Q, De ng B, Luo J, Tao J (2018) Extraction of scandium from scandium-rich material derived from bauxite ore residues[J]. Hydrometallurgy 176:62–68

12. Liu C, Ma S, Zheng S, Luo Y, Ding J, Wang X, Zhang Y (2018) Combined treatment of red mud and coal fly ash by a hydro- chemical process[J]. Hydrometallurgy, S0304386X17304681
13. Liu S, Li Z, Li Y, Cao W (2018) Strength properties of bayer red mud stabilized by lime-fly ash using orthogonal experiments. Constr Build Mater 166:554–563
14. Mukiza E, Zhang L, Liu X, Zhang N (2019) Utilization of red mud in road base and subgrade materials: A review[J], vol 141. Resources, Conservation & Recycling, pp 187–199
15. Naga, Babu A, Km GV, K., K., and K., R (2018) Removal of fluoride from water using H_2O_2 -treated fine red mud doped in zn-alginate beads as adsorbent. J Environ Chem Eng 6(1):906–916
16. Narayanan RPN, Kazantzis NK, Emmert MH (2017) Selective Process Steps for the Recovery of Scandium from Jamaican Bauxite Residue (Red Mud)[J]. ACS Sustainable Chemistry & Engineering. acssuschemeng.7b03968
17. Ofori P, Nguyen AV, Firth B, Mcnally C, Ozdemir O (2011) Shear-induced floc structure changes for enhanced dewatering of coal preparation plant tailings[J]. Chem Eng J 172(2):914–923
18. Petrak M, Hiller E, Sottnik P, Jurkovic L, Volekova B, Toth R, Vozar J (2013) Geochemical characterization and evaluation of a neutral, low-sulfide/high-carbonate tailings impoundment, markusovce (slovakia) [J]. International Multidisciplinary Scientific GeoConference Surveying Geology and Mining Ecology Management, 1:505–512
19. Pepper RA, Couperthwaite SJ, Millar GJ (2018) Re-use of waste red mud: Production of a functional iron oxide adsorbent for removal of phosphorous[J]. J Water Process Eng 25:138–148
20. Sabat AK, Mohantab S (2015) Efficacy of dolime fine stabilized red mud-fly ash mixes as subgrade material. ARPN J Eng Appl Sci 10:5919–5923
21. Shamsai A, Pak A, Bateni SM, Ayatollahi SAH (2007) Geotechnical characteristics of copper mine tailings: a case study[J]. Geotech Geol Eng 25(5):591–602
22. Shamshad A, Das SK, Rao BH (2017) Characterization of coarse fraction of red mud as a civil engineering construction material [J]. J Clean Prod 168:679–691
23. Shu Z, Liu S, Song B, Pan J (2012) A comparison on tailings treatment and disposal of aba lead-zinc concentrator[J]. Adv Mater Res 511:32–35
24. Yuan XM, Xiong F et al (2008) Occurrence state of fluorine in red mud [J]. Environ Monit China 24(4):46–49 (in Chinese)
25. Wang X, Ma J, Zhang L, Yang J (2018) Radioactive Element Distribution Characteristics of Red Mud based Field Road Cement before and after Hydration [J].Journal of Wuhan University of Technology-Mater. Sci. Ed., (2):452–458
26. Wang X, Luo Z, Zhang L, Rong H, Yang J (2016) Utilization of red mud as raw material in the production of field road cement [J]. J Wuhan Univ Technology-Mater Sci Ed 31(4):877–882
27. Zhang H, Li H, Zhang Y, Wang D, Harvey J, Wang H (2018) Performance enhancement of porous asphalt pavement using red mud as alternative filler [J]. Constr Build Mater 160:707–713

Figures

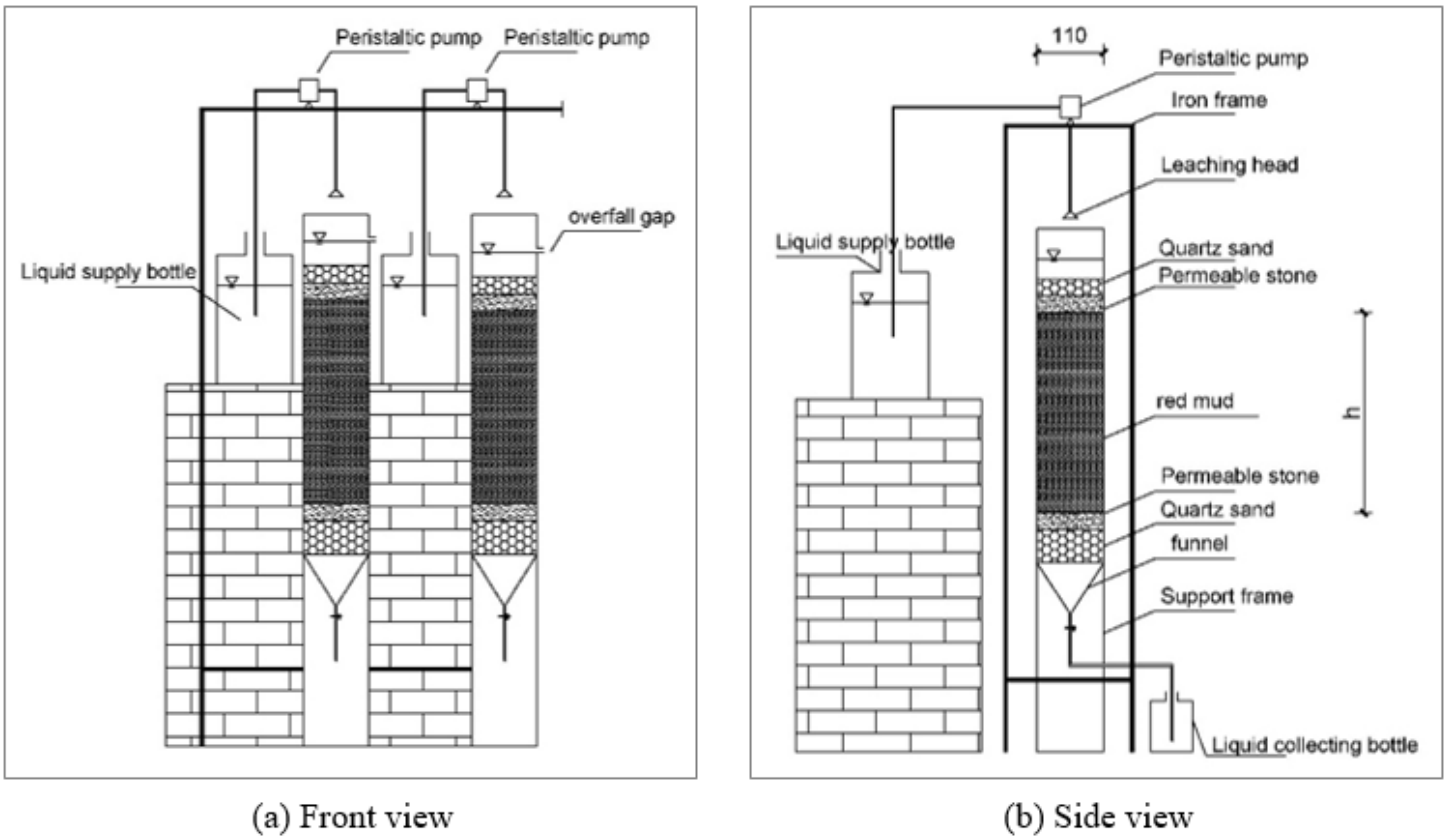

Figure 1

Partial structure diagram of leaching device (including a, b)

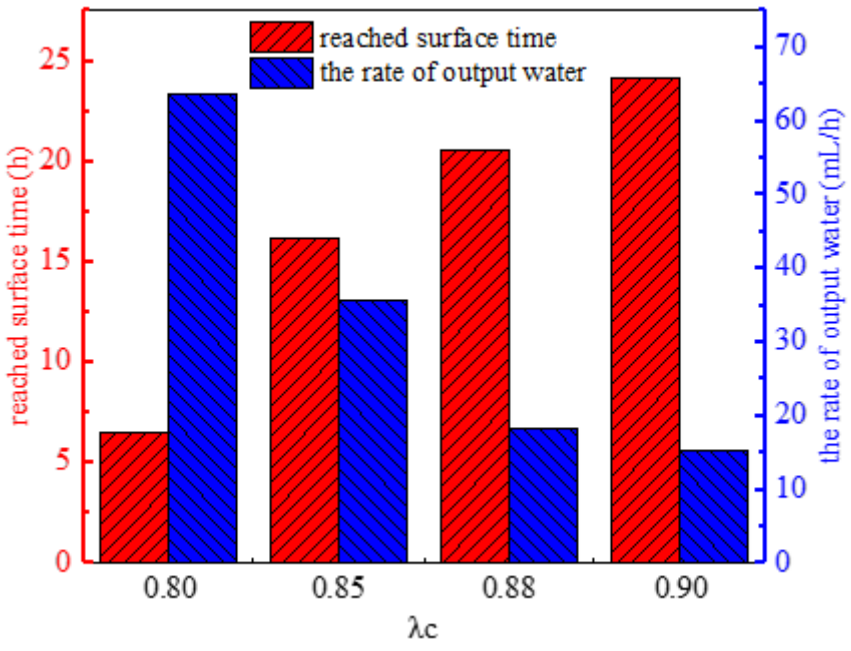

Figure 2

The change of effluent time and rate with compactness

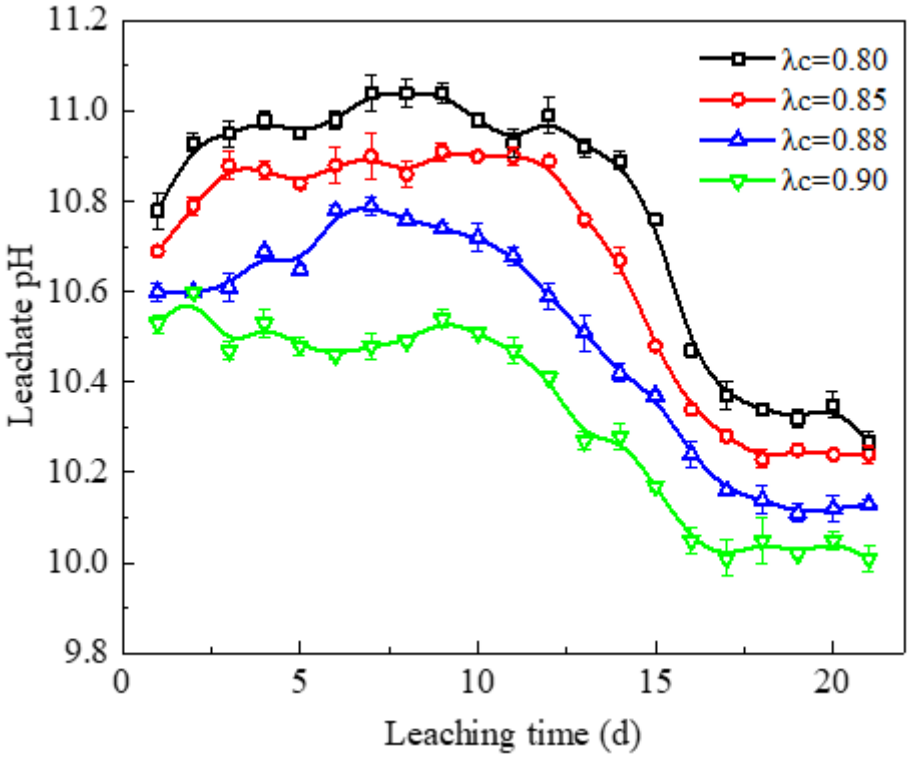

Figure 3

Change of pH value of exudate with leaching time

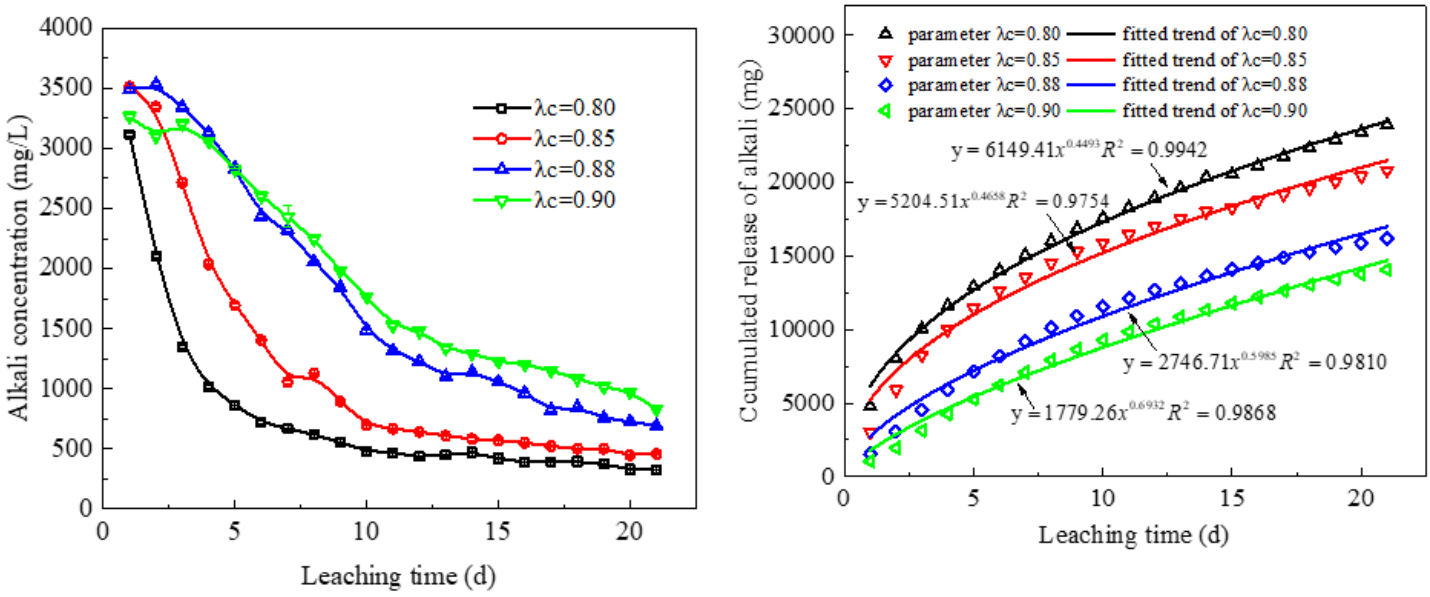

(a) Variation of alkali concentration in exudate with leaching time

(b) Variation of alkali release with leaching time

Figure 4

Alkali release characteristic diagram (including a, b)

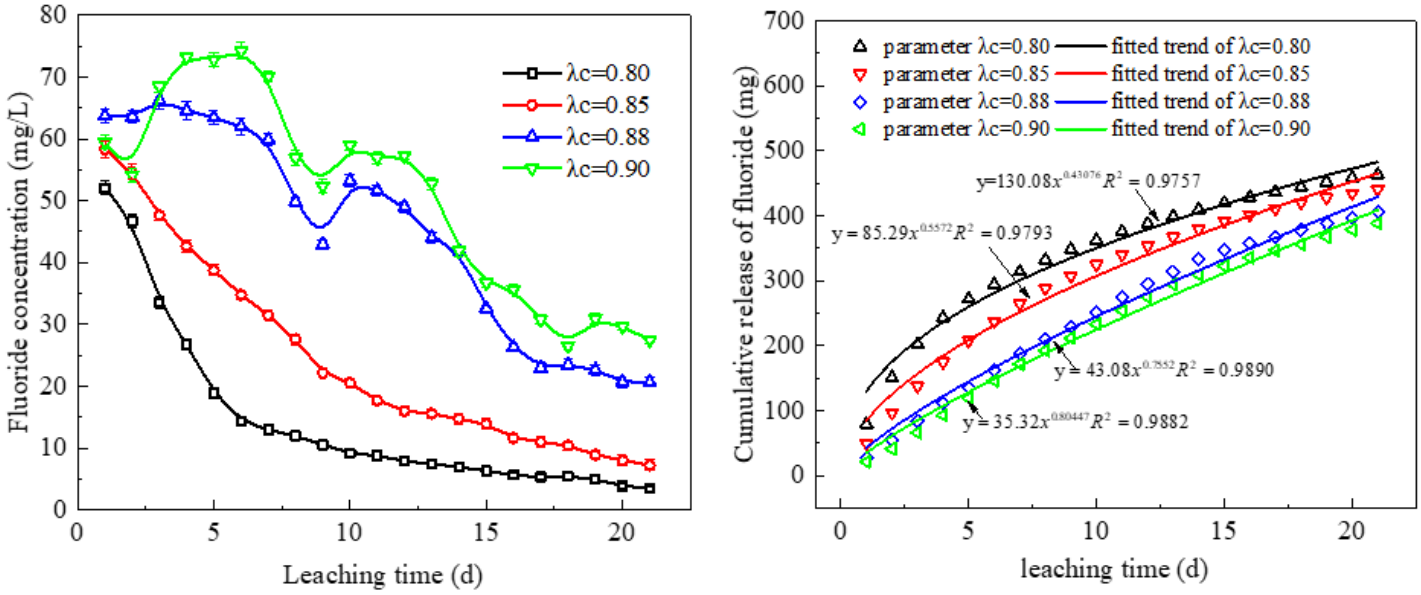

(a) Variation of fluoride concentration in exudate with leaching time

(b) Variation of fluoride cumulative release with leaching time

Figure 5

Fluoride release characteristic diagram (including a, b)

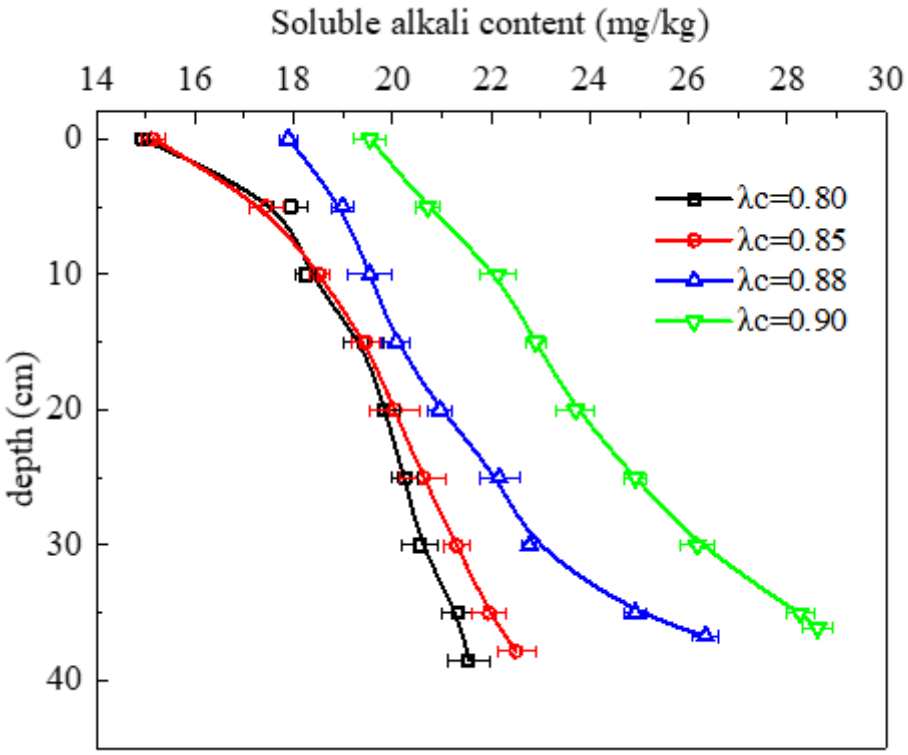

Figure 6

Variation of soluble alkali content in leached red mud with the depth of leaching column

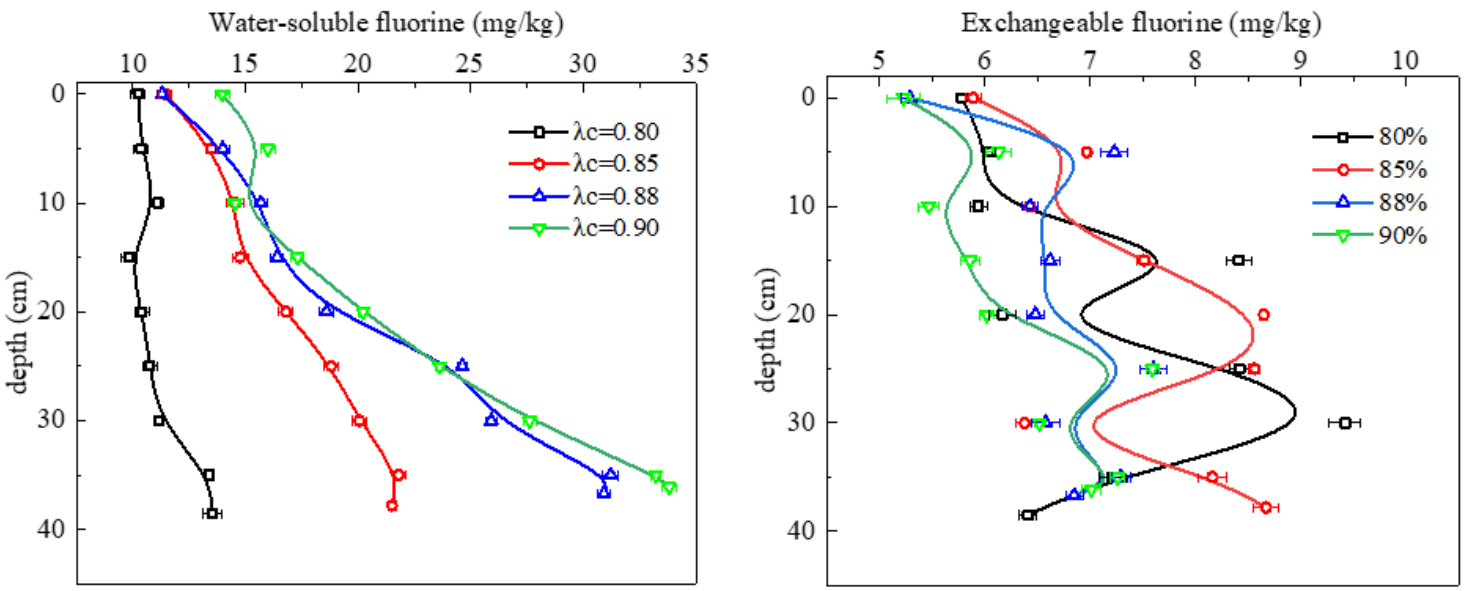

(a) Diagram of Ws-F variation with depth

(b) Diagram of Es-F variation with depth

Figure 7

Changes of Ws-F and Es-F contents in leached red mud with the depth of leaching column (including a, b)